Novel color-tunable $Gd_2O_2CN_2:Tb^{3+}$, Eu^{3+} phosphors: Characterization and photoluminescence properties

Shuanglong Yuan[1*], Luting Wang[1], Yunxia Yang[1], Francois Cheviré[2], Franck Tessier[2], Guorong Chen[1]

[1]Key Laboratory for Ultrafine Materials of Ministry of Education, School of Materials Science and Engineering, East China University of Science and Technology, Shanghai 200237, China

[2]Institut des Sciences Chimiques de Rennes (UMR CNRS 6226), équipe Verres et Céramiques, Université de Rennes 1, F-35042 Rennes cedex, France

[*]Corresponding author : Shuanglong@ecust.edu.cn

Abstract

In this paper, color-tunable $Gd_2O_2CN_2:Tb^{3+},Eu^{3+}$ phosphors were obtained by co-doping Eu^{3+} and Tb^{3+} ions into $Gd_2O_2CN_2$ host and singly varying the Eu^{3+} doping concentration. The characteristics of the crystal structure, photoluminescence lifetime and photoluminescence of Tb^{3+},Eu^{3+} single-doped and Tb^{3+} and Eu^{3+} co-doped $Gd_2O_2CN_2$, were carefully investigated by XRD, FTIR, PL decay curves and photoluminescence (PL). The results indicated that Tb^{3+} single-doped $Gd_2O_2CN_2$ phosphor show a green emission, and by increasing Eu^{3+} content, $Gd_2O_2CN_2:Tb^{3+}$, Eu^{3+} phosphors emit green to orange and then to red light under the excitation of 379nm.

Keywords: Photoluminescence; $Gd_2O_2CN_2:Tb^{3+}$, Eu^{3+}; color-tunable phosphors

1. Introduction

During the past few years, rare earth oxycyanamide compounds as host materials have received much attention due to their outstanding luminescence properties when doped with rare-earth ions[1-3]. The structures of $RE_2O_2CN_2$ and RE_2O_2S are closely related [4] and previous work has

shown that the luminescence properties of $RE_2O_2S:Eu^{3+}$ (RE=Gd and Y) and $RE_2O_2CN_2:Eu^{3+}$ (RE=Gd and Y) are quite similar [5, 6]. Therefore, such oxycyanamide compounds are considered to be efficient host candidates for rare-earth activators ions such as Eu^{3+} and Tb^{3+} for instance. Eu^{3+} is considered as an important activator ion with red emission corresponding to the transition of $^5D_0$-^7F_J (J=1-6) [7]. The emission of Tb^{3+} is due to the transition between the emitting states of ^5D_j and the excited states of ^7F_j, and the main intense green emission is attributed to the transition of $^5D_4$-$^7F_5$ which is located at ca. 543nm[8].

In the previous study, we have reported the strong red emission of Eu^{3+} doped $Gd_2O_2CN_2$ phosphors [9]. In this work, we report a new color tunable phosphor $Gd_2O_2CN_2$: Tb^{3+}, Eu^{3+}. A series of Tb^{3+}, Eu^{3+} singly-doped and Tb^{3+}-Eu^{3+} co-doped phosphors were successfully prepared by classical solid state reaction at low firing temperature(750 °C). The emitting color of $Gd_2O_2CN_2$: Tb^{3+}, Eu^{3+} phosphors can be tuned from green to orange and then to red by singly varying the doping concentration of Eu^{3+}. The mechanism of energy transfer between Tb^{3+} and Eu^{3+} was investigated, and the results show that Eu^{3+}/Tb^{3+} co-doped $Gd_2O_2CN_2$ phosphors could serve as potential phosphors for NUV LEDs.

2. Experimental

Powder samples with the general formula $Gd_{2-x}Tb_xO_2CN_2$ [x=0.03(T-1), 0.05(T-2), 0.07(T-3), 0.12(T-4), 0.15(T-5) and 0.20 (T-6)], $Gd_{1.90}Eu_{0.1}O_2CN_2$（GOCN-4）and $Gd_{1.85-y}Tb_{0.15}Eu_yO_2CN_2$ [y=0.02(ET-1), 0.04(ET-2), 0.06(ET-3), 0.08(ET-4), 0.10(ET-5), 0.15(ET-6) were prepared by solid state reaction. High purity GdF_3 (99.99%), Eu_2O_3 (99.99%), Tb_4O_7 (99.99%), Li_2CO_3 (99.99%), and active carbon (CARBIO 12 SA—ref: C1220 G 90) as the raw materials were thoroughly mixed and fired at 600 °C for 9 h, then 750 °C for 12 h under NH_3 atmosphere. The

detailed synthesis routes can be found in literature [9].

Powder X-ray diffraction (XRD) data were recorded using a Bruker AXS D8 Advance diffractometer (Voltage 50 kV, current 40 mA, Cu-Ka). Photoluminescence (PL) and photoluminescence excitation (PLE) spectra were measured by a Fluorolog-3-P UV-vis-NIR fluorescence spectrophotometer (Jobin Yvon, longjumeau, France) with a 450 W Xenon lamp as the excitation source. The decay curves of Tb^{3+} emission was performed by FLSP920 (Edinburgh Instruments). The FTIR spectrum was measured in transmission mode using a KBr standard (Bruker, Model vector 22). The color chromaticity coordinates were obtained according to Commission Internationale de I'Eclairage (CIE) using Radiant Imaging color calculator software.

3. Results and discussion

As shown in Figure 1, the XRD patterns of the Tb^{3+} and/or Eu^{3+} activated $Gd_2O_2CN_2$ samples can be readily indexed as a trigonal phase and identified as $Gd_2O_2CN_2$ with the space group P-3m1 according to the JCPSQ database(PDF#49-1169). Considering the similar coordinated environment, electronegativity and ionic radii of Gd^{3+} (r=0.100nm, CN=7), Tb^{3+} (r=0.098nm, CN=7) and Eu^{3+}(r=0.101nm, CN=7) ions, doping Tb^{3+} and Eu^{3+} does not result in any phase transformation and only has minor influence to the crystal structure.

Figure 2 shows the IR spectra of GOCN-4，ET-5 and T-5. IR spectra for ET-5 and T-5 both have the intense peaks at 2080 and 652 cm^{-1}. In our previous study we reported that the typical absorption peaks in the vicinity of 2010 and 652 cm^{-1} in the GOCN-4 were respectively assigned to the ν_2 (bending vibration) and ν_3 (asymmetric stretching vibration) modes of the CN_2^{2-} ion [9]. Hence, the IR spectra also indicate that CN_2^{2-} ions contained in Eu^{3+}, Tb^{3+} single-doped and Eu^{3+}-Tb^{3+} co-doped $Gd_2O_2CN_2$ samples.

Figure 3 illustrates the excitation (monitored at 543 nm) and emission (excited by 280, 313 and 365 nm) spectra of the T-5 sample (7.5 at. % Tb^{3+}). The excitation spectrum (Fig. 3a) exhibits a broad and intense band in the range from 250 to 300 nm with a peak at around 280 nm. This broad band is attributed to $4f^8$-$4f^75d^1$ transitions of Tb^{3+} ions. The other excitation bands at longer wavelengths, are located at 307 nm ($^5H_5 \rightarrow {}^7F_6$), 313 nm ($^5H_5 \rightarrow {}^7F_5$) and 350-380nm (transitions from $^7F_4$, $^7F_3$ to $^5H_7$, $^5D_0$, $^5D_1$).The emission spectra of T-5 (Fig. 3b) at different excitation wavelengths are very similar both in shape and relative intensities. The strongest peak split into two at 543 and 550 nm corresponds to the $^5D_4 \rightarrow {}^7F_5$ transition, while the peaks at 487 and 495nm, 587nm, and 622nm respectively originate from the $^5D_4 \rightarrow {}^7F_6$, $^5D_4 \rightarrow {}^7F_4$ and $^5D_4 \rightarrow {}^7F_3$ transitions of Tb^{3+} ions.

The excitation (monitored at 543nm) and emission (monitored at 280nm) spectra of $Gd_{2-x}Tb_xO_2CN_2$ with varying Tb^{3+} concentrations (x=0.03, 0.05, 0.07, 0.12, 0.15 and 0.20) are shown in Fig. 4. With the increase of doped Tb^{3+} ions concentration, the excitation and the emission intensity increases gradually ranging from 1.5 to 7.5 at. % and decreases from 7.5 to 10 at. %, which is in accordance with Eu^{3+} doped $Gd_2O_2CN_2$ in previous work [9]. Considering the mechanism of energy transfer in phosphors, the concentration quenching can be explained in more details by the critical distance (R_c) between Tb^{3+} ions which can be calculated by Eq. (1) [10]:

$$R_c = 2 \times (3V / 4\pi X_c N)^{1/3} \quad (1)$$

Where V (101.9 $Å^3$) is the volume of the unit cell, X_c (0.075) is the critical concentration of Tb^{3+} ions and N (2) is the number of lattice sites in the unit cells that can be occupied by Tb^{3+} ions.Therefore, R_c between Tb^{3+} ions is calculated to be 10.907 Å .

PL and PLE spectra of singly-doped Eu^{3+} (GOCN-4, 5 at. %) or Tb^{3+} (T-5, 7.5 at. %) and

Eu^{3+}/Tb^{3+} (ET-1, 1at. %/ 7.5 at. %) co-doped $Gd_2O_2CN_2$ phosphors are presented in Fig. 5. The excitation spectrum of GOCN-4 exhibits a broad and intense band in the range from 250 to 350 nm with a peak at around 300 nm, which is attributed to the ligand-to-metal charge transfer between O^{2-} and Eu^{3+}. The weak excitation bands at longer wavelength corresponding to the 4f-4f transitions of Eu^{3+} are located at 379nm ($^7F_0 \rightarrow {}^5G_2$), 395nm ($^7F_0 \rightarrow {}^5L_6$), 467nm ($^7F_0 \rightarrow {}^5D_2$). Upon excitation at 300nm, the emission spectrum shows two strong peaks at 614 and 626 nm which originate from the $^5D_0 \rightarrow {}^7F_2$ transition of Eu^{3+}. Fig. 5 (b) shows the excitation and emission spectra of T-5, an intensive broad excitation band with the maximum at 280nm and other peaks at 313 and 379nm are observed. Upon the excitation at 280nm, the emission spectrum shows a strong peak at 543nm which is attributed to the transition $^5D_4$-$^7F_5$ of Tb^{3+}. Fig. 5 (c) shows the excitation spectra of ET-1 monitored at 626 and 543nm, the excitation band at around 379nm can be observed in both excitation spectra. The emission spectrum of ET-1 shows typical peaks at 543nm that originated from transition $^5D_4$-$^7F_5$ of Tb^{3+} and at 614 and 626nm from transition $^5D_0 \rightarrow {}^7F_2$ of Eu^{3+}.

The emission spectra of $Gd_{1.85-y}Tb_{0.15}Eu_yO_2CN_2$ ($0 \leq y \leq 0.15$) are illustrated in Fig. 6. All samples exhibit two prominent peaks peaking at 543 and 626nm under 379nm excitation. By increasing the concentration of Eu^{3+}, the emission intensities of Tb^{3+} at 543nm decrease remarkably while the emission intensity of Eu^{3+} at 626nm initially increases and then reaches a maximum at y=0.10, then decreases due to the concentration quenching. Therefore, we can speculate about the existence of energy transfer from Tb^{3+} to Eu^{3+} cations, such an energy transfer has also been observed in Y_2O_3[11], $Ca_8MgLu(PO_4)_7$ [12]and $SrMg_2La_2W_2O_{12}$ host materials[13].

To further certify the energy transfer from Tb^{3+} to Eu^{3+} ions in $Gd_2O_2CN_2$ host matrix, the PL decay curves were measured (excited at 379nm and monitored at 543nm) and the lifetimes of

different samples were calculated. Fig. 7 shows the decay curves of Tb^{3+} ions which can be well fitted to a double-exponential function as the following equation [14]:

$$I = I_0 + A_1 \exp(-t/\tau_1) + A_2 \exp(-t/\tau_2) \quad (1)$$

Where I is the luminescent intensity at the time of t and I_0 is the luminescent intensity at the time of 0; A_1 and A_2 are fitting parameters; τ_1 and τ_2 are rapid and slow lifetimes for exponential components, respectively. Based on these parameters, the average lifetime of Tb^{3+} ions with different Eu^{3+} concentration can be calculated by the following equation:

$$\tau = (A_1\tau_1^2 + A_2\tau_2^2) / (A_1\tau_1 + A_2\tau_2) \quad (2)$$

The effect of Eu^{3+} content on the calculated Tb^{3+} ions lifetimes was shown in the Fig. 7 inset, the decay lifetime of Tb^{3+} ions decrease with increasing Eu^{3+} concentration, which strongly supported the energy transfer from Tb^{3+} ions to Eu^{3+} ions.

Table 1 summarizes the CIE chromaticity coordinates of $Gd_{1.85-y}Tb_{0.15}Eu_yO_2CN_2$ ($0 \le y \le 0.20$) phosphors under the excitation at 379nm, Figure 8 also gives the CIE chromaticity coordinates, and it is interesting to notice that with the increasing of Eu^{3+} ions concentration, the CIE chromaticity coordinates shift from (0.3134, 0.5454) to (0.5682, 0.3322), the emitting color turned from green to red accordingly. The inset of Fig. 8 also shows the digital photos of $Gd_{1.85}Tb_{0.15}O_2CN_2$ (a), $Gd_{1.83}Tb_{0.15}Eu_{0.02}O_2CN_2$ (b) and $Gd_{1.70}Tb_{0.15}Eu_{0.15}O_2CN_2$ (g) phosphors under excitation at 379nm light. With the development of chip technology, high-performance InGaN-based 380 nm UV LEDs are fabricated [15] and commercially available NUV InGdN LED chip from 375 to 380nm is more and more common. Therefore, Eu^{3+}, Tb^{3+} co-doped $Gd_2O_2CN_2$ phosphors may have potential applications for NUV LEDs.

4. Conclusion

In this paper, Eu^{3+}, Tb^{3+} singly doped and Eu^{3+}-Tb^{3+} co-doped $Gd_2O_2CN_2$ phosphors were successfully prepared by classical solid-state reaction. The Tb^{3+} doped $Gd_2O_2CN_2$ phosphors exhibit a characteristic green emission with the strong peak at 543nm. The optimized Tb^{3+} concentration of $Gd_2O_2CN_2$:Tb^{3+} is 7.5 at. %. When Eu^{3+} and Tb^{3+} were co-doped into $Gd_2O_2CN_2$, an efficient energy transfer from Tb^{3+} to Eu^{3+} occurred and thus by only increasing the doping concentration of Eu^{3+}, it becomes possible to tune the emission color from green to orange and then to red under the excitation at 379nm.

Acknowledgement

This project has been supported by the National Natural Science Foundation of China (No.51502091), and the Fundamental Research Funds for the Central Universities (WD1314055, WD1313009).

References

1 E. Sailynoja, M. Lastusaari, J. Holsa, P. Porcher, "Luminescence of a novel rare earth oxycompound $La_2O_2CN_2$:Eu^{3+}," Journal of Luminescence.**72-74** 201-203(1997).

2 J. Holsä , R.-J. Lamminmäki , M. Lastusaari, P. Porcher, and E. Säilynoja, "Crystal field effect in RE -doped lanthanum oxycyanamide, $La_2O_2CN_2$:RE^{3+}(RE =$Pr^{3+}$and Eu^{3+})," J. Alloys Compd. **275–277**, 402–406 (1998).

3 T. Takeda, N. Hatta, and S. Kikkawa, "Gel nitridation preparation and luminescence property of Eu-doped $RE_2O_2CN_2$ (RE =La and Gd) phosphor," Chem. Lett. **35**, 988-989 (2006).

4 H.-J. Meyer, "Solid state metathesis reactions as a conceptual tool in the synthesis of new materials," Dalton Transactions. **26**, 5973-5982(2010).

5 T. Hang, Q. Liu, D. L. Mao, C. K. Chang, "Long lasting behavior of Gd_2O_2S:Eu^{3+} phosphor

synthesized by hydrothermal routine," Materials Chemistry and Physics. **107**, 142–147(2008).

6 J. Sindlinger, J. Glaser, H. Bettentrup, T. Jüstel, and H.-J. Meyer, "Synthesis of $Y_2O_2(CN_2)$ and luminescence properties of $Y_2O_2(CN_2)$: Eu," Z. Anorg. Allg. Chem. **633**, 1686-1690 (2007).

7 S. H. Yang, C. H. Yen, C. M. Lin, P. J. Chiang, "Energy transfer mechanism and luminescent properties of color tunable $LaPO_4$:Tm,Eu phosphor," Ceramics International.**41**, 8211–8215(2015).

8 T. Wang, X. H. Xu, D. C. Zhou, J. B. Qiu, X. Yu, "Tunable color emission in $K_3Gd(PO_4)_2$:Tb^{3+},Sm^{3+} phosphor for n-UV white light emitting diodes," Journal of rare earths. **33**,361-365(2015).

9 L. T. Wang, S. L. Yuan, Y. X. Yang, F. Chevire, F. Tessier, and G. R. Chen, "Luminescent properties of novel red-emitting phosphor: $Gd_2O_2CN_2$:Eu^{3+}," Optical Materials Express. **5**,2616-2624(2015).

10 G. Blasse, "Energy transfer in oxidic phosphors," Phys. Lett. A, **28**, 444-445 (1968).

11 Z. L. Liu, L. X. Yu, Q. Wang, Y. C. Tao, H. Yang, "Effect of Eu, Tb codoping on the luminescent properties of Y_2O_3 nanorods," Journal of Luminescence. **131**,12-16(2011).

12 F. Y. Xie, J. H. Li, Z. Y. Dong, D. W. Wen, J. X. Shi, J. Yan, and M. M. Wu, "Energy transfer and luminescent properties of $Ca_8MgLu(PO_4)_7$:Tb^{3+}/Eu^{3+} as a green-to-red color tunable phosphor under NUV excitation," RSC Advances. **5**, 59830-59836(2015).

13 K. Pavani, J. S. Kumar, L. R. Moorthy, "Photoluminescence properties of Tb^{3+} and Eu^{3+} ions co-doped $SrMg_2La_2W_2O_{12}$ phosphors for solid state lighting applications," Journal of Alloys and Compounds.**586**,722-729(2014).

14 Y. Q. Zhai, M. Wang, Q. Zhao, J. B. Yu, X. M. Li. Fabrication and luminescent properties of

$ZnWO_4$:Eu^{3+}, Dy^{3+} white light-emitting phosphors. Journal of luminescence, 2016, 172: 161-167.

15 S. C. Huang, D.-S. Wuu, P. Y. Wu, and S.-H. Chan, "Improved output power of 380nm InGaN-Based LEDs using a heavily Mg-Doped GaN Insertion layer technique," IEEE Journal of Selected Topics in Quantum electronics. **15**, 1132-1136(2009).

FIG. 1. XRD patterns of $Gd_{1.9}Eu_{0.1}O_2CN_2$, $Gd_{1.75}Tb_{0.15}Eu_{0.1}O_2CN_2$ and $Gd_{1.85}Tb_{0.15}O_2CN_2$ (the standard data of $Gd_2O_2CN_2$ (PDF#49-1169) is shown as reference)

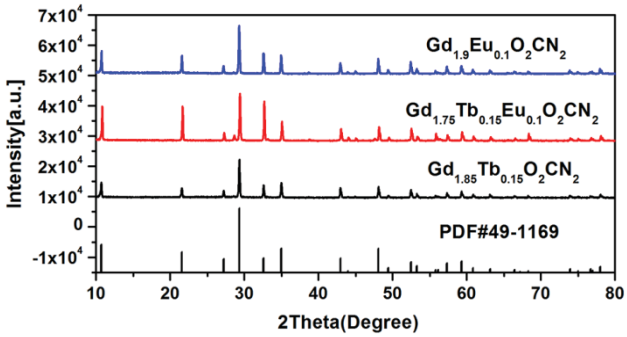

FIG. 2. FTIR spectra of $Gd_{1.9}Eu_{0.1}O_2CN_2$, $Gd_{1.75}Tb_{0.15}Eu_{0.1}O_2CN_2$ and $Gd_{1.85}Tb_{0.15}O_2CN_2$ samples

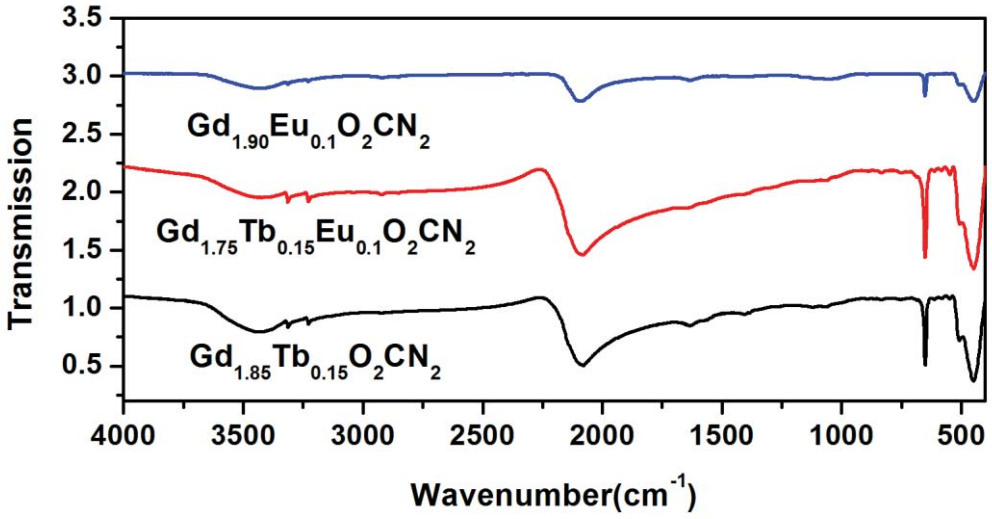

FIG. 3. Excitation (a) and Emission (b) spectra of the $Gd_{1.85}Tb_{0.15}O_2CN_2$ sample. The right inset is the photograph image of the Tb^{3+}-doped sample being excited by the 280nm lights.

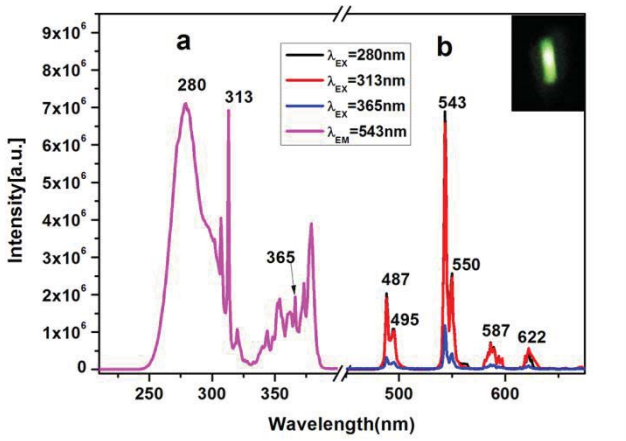

FIG. 4. Excitation (a) and emission (b) spectra of $Gd_{2-x}Tb_xO_2CN_2$ (x=0.03, 0.05, 0.07, 0.12, 0.15, 0.200) samples. The inset is the dependence of its PL intensity on the Tb^{3+} content in the $Gd_2O_2CN_2$ matrix.

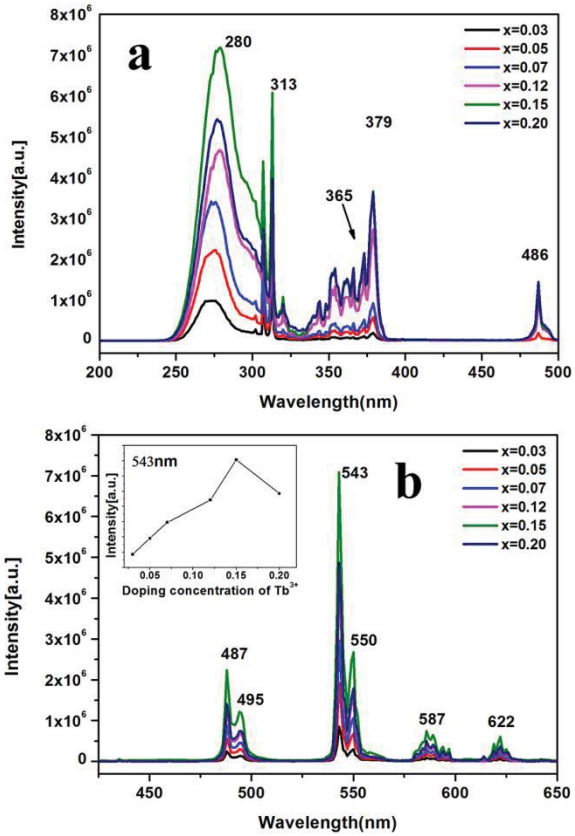

FIG. 5. Excitation and emission spectra of $Gd_{1.90}Eu_{0.10}O_2CN_2$ (a), $Gd_{1.85}Tb_{0.15}O_2CN_2$ (b) and $Gd_{1.83}Eu_{0.02}Tb_{0.15}O_2CN_2$ (c)

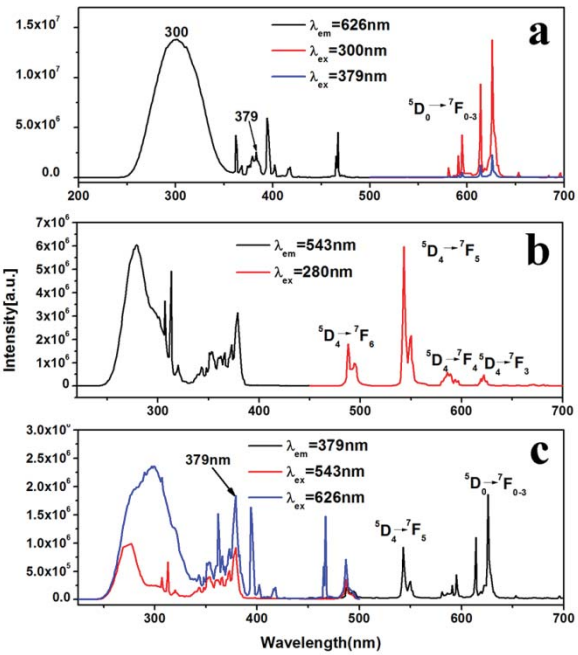

FIG. 6. Emission spectra of $Gd_{1.85-y}Tb_{0.15}Eu_yO_2CN_2$ (y=0, 0.02, 0.04, 0.06, 0.08, 0.10, 0.15) samples under the excitation wavelength of 379nm

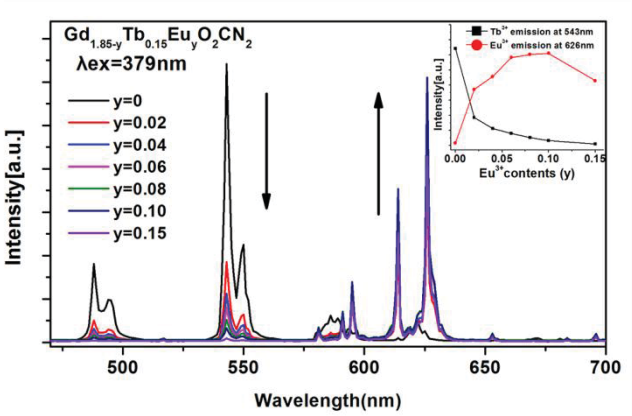

FIG. 7. Representative decay curves for the luminescence of Tb^{3+} in $Gd_{1.85}Tb_{0.15}O_2CN_2$, $Gd_{1.83}Tb_{0.15}Eu_{0.02}O_2CN_2$ and $Gd_{1.81}Tb_{0.15}Eu_{0.04}O_2CN_2$. The inset shows the lifetime of Tb^{3+} as a function of Eu^{3+} concentration in $Gd_2O_2CN_2$ host matrix (excited at 379 nm and monitored at 543 nm).

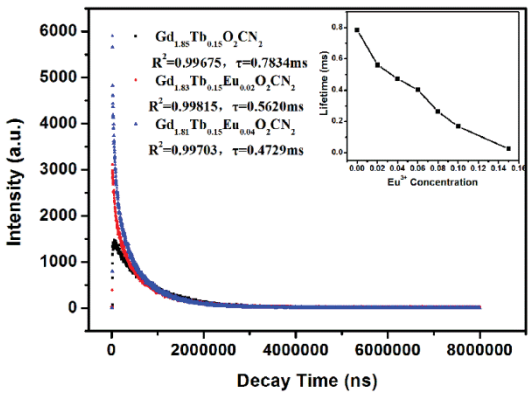

FIG. 8. CIE chromaticity coordinate digram of $Gd_{1.85-y}Tb_{0.15}Eu_yO_2CN_2$ (y=0, 0.02, 0.04, 0.06, 0.08, 0.10, 0.15) samples under the excitation at 379nm (the inset shows the digital photos of the $Gd_{1.85}Tb_{0.15}O_2CN_2$ (a), $Gd_{1.83}Tb_{0.15}Eu_{0.02}O_2CN_2$ (b) and $Gd_{1.70}Tb_{0.15}Eu_{0.15}O_2CN_2$ (g) phosphors under the excitation of 379nm light

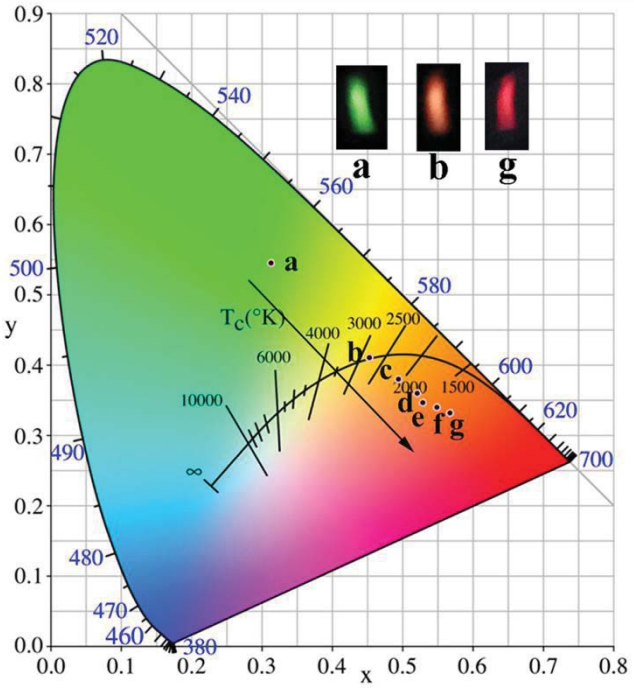

Table 1 CIE chromaticity coordinates for $Gd_{1.85-y}Tb_{0.15}Eu_yO_2CN_2$ (y=0, 0.02, 0.04, 0.06, 0.08, 0.10, 0.15) samples

Sample no.	Sample composition(y)	CIE coordinates (x,y)
a (T-5)	y=0	(0.3134, 0.5454)
b (ET-1)	y=0.02	(0.4534, 0.4112)
c (ET-2)	y=0.04	(0.4953, 0.3794)
d (ET-3)	y=0.06	(0.5216, 0.3596)
e (ET-4)	y=0.08	(0.5289, 0.3469)
f (ET-5)	y=0.10	(0.5493, 0.3405)

g (ET-6)	y=0.15	(0.5682, 0.3322)